Equation-Free Multiscale Computation: Algorithms and Applications

Ioannis G. Kevrekidis[1] and Giovanni Samaey[2]

[1]Department of Chemical Engineering and Program in Applied and Computational Mathematics, Princeton University, Princeton, New Jersey 08544; email: yannis@princeton.edu

[2]Department of Computer Science, Katholieke Universiteit Leuven, 3001 Leuven, Belgium, email: giovanni.samaey@cs.kuleuven.be

Annu. Rev. Phys. Chem. 2009. 60:321–44

The *Annual Review of Physical Chemistry* is online at physchem.annualreviews.org

This article's doi:
10.1146/annurev.physchem.59.032607.093610

0066-426X/09/0505-0321$20.00

Key Words

complex systems, equation-free methods, simulation, bifurcation analysis, patch dynamics

Abstract

In traditional physicochemical modeling, one derives evolution equations at the (macroscopic, coarse) scale of interest; these are used to perform a variety of tasks (simulation, bifurcation analysis, optimization) using an arsenal of analytical and numerical techniques. For many complex systems, however, although one observes evolution at a macroscopic scale of interest, accurate models are only given at a more detailed (fine-scale, microscopic) level of description (e.g., lattice Boltzmann, kinetic Monte Carlo, molecular dynamics). Here, we review a framework for computer-aided multiscale analysis, which enables macroscopic computational tasks (over extended spatiotemporal scales) using only appropriately initialized microscopic simulation on short time and length scales. The methodology bypasses the derivation of macroscopic evolution equations when these equations conceptually exist but are not available in closed form—hence the term equation-free. We selectively discuss basic algorithms and underlying principles and illustrate the approach through representative applications. We also discuss potential difficulties and outline areas for future research.

1. INTRODUCTION

Closure: relation embodying the effect of unmodeled variables on those variables (observables) in terms of which the (coarse) model is formulated (closed)

Coarse time-stepper: three-step procedure to observe the evolution in time of the coarse states modeled by an unknown coarse equation: lift, simulate with the fine-scale model, and restrict (observe)

Lifting: one-to-many mapping from a coarse to a fine-scale state; reinitialization of the fine-scale model consistent with a prescribed coarse state

Restriction: mapping from a fine scale to a coarse state; observation (estimation) of the coarse state from the corresponding fine-scale state

Inner/outer solver: fine-scale/coarse components in two-tier equation-free computations

In a wide range of chemical, physical, and biological systems, macroscopic, coherent behavior emerges from interactions between microscopic entities (molecules, cells, individuals in a population) among themselves and with their environment. In many cases, a macroscopic model (such as the Navier-Stokes equations for fluid flow or a reaction-diffusion equation) has been formally derived that quantitatively describes behavior at this level. These models typically take the form of conservation laws (species, mass, momentum, energy) closed through phenomenological constitutive equations (reaction rates as functions of concentrations, viscous stresses as functionals of velocity gradients). Mathematical techniques including homogenization, averaging, renormalization, and the theory of inertial manifolds (1–4), as well as methods of systematic coarse graining (e.g., 5), are available to derive macroscopic equations from an underlying fine-scale description, underpinning many successful explicit closures in equilibrium and nonequilibrium statistical mechanics (e.g., 6–12).

Increasingly, however, one encounters complex systems that can only be modeled with sufficient accuracy at a microscopic, fine scale; in such cases, although one observes the emergence of coarse-scale, macroscopic behavior in practice, modeling it directly may be impossible or impractical without simplifying assumptions that are hard to justify. Non-Newtonian fluid flow (13), chemotaxis (14), and porous media transport (15) are but a few typical examples. Performing macroscopic computational tasks with microscopic models is often infeasible: Direct simulation over the full spatiotemporal domain of interest can be computationally prohibitive. Moreover, additional modeling tasks, such as numerical bifurcation analysis, are often impossible to perform on the microscopic model directly. A coarse steady state may not imply a steady state for the fine-scale system as, for instance molecules do not stop moving when the gas density or pressure equilibrate.

This article reviews a multiscale approach (16) to performing coarse-level computational tasks for systems that are modeled at a (much) finer scale (for an earlier review, see 17). In many cases, the explicit derivation of macroscopic equations can be circumvented by using short bursts of appropriately initialized microscopic simulation. A key tool is the coarse time-stepper, discussed in Section 2, which implements a time step of an unavailable macroscopic model as a three-step procedure: (*a*) lifting (i.e., the creation of initial conditions for the fine-scale model, conditioned upon the coarse state at t^*), (*b*) simulation (using the fine-scale model, over a time interval $[t^*, t^* + \delta t]$), and (*c*) restriction [i.e., the observation (estimation) of the coarse state at $t^* + \delta t$].

Once a coarse time-stepper is available, one can build a direct bridge between fine-scale simulation and algorithms of traditional continuum numerical analysis, such as numerical bifurcation analysis, optimization, control, and even accelerated coarse-scale simulation. Traditionally, a coarse-level solver (which we call the outer solver) evaluates the required information (time derivatives, the action of Jacobians) using explicit formulae from the coarse model. In the equation-free approach, the outer solver uses appropriately initialized computational experiments with the fine-scale (inner) simulator to obtain a closure on demand. The analogy with matrix-free methods in numerical linear algebra (18) provides another reason for the term equation-free; it emphasizes that the coarse-level equations are never constructed explicitly in closed form. In Section 3, we discuss time-stepper-based coarse bifurcation analysis. We then show how to accelerate coarse evolution computations using the fine-scale simulator in a small fraction of the space-time domain of interest, discussing coarse projective integration (Section 4) and patch dynamics schemes (Section 5). Section 6 contains selected illustrative applications. Section 7 presents potential difficulties and an outlook for further research.

The equation-free framework relates to, and borrows ideas from, a long history of (computational) multiscale approaches. Without aspiring to completeness, we mention Phillips and coworkers' (19–21) quasi-continuum methods, in which the quantities required in solving for macroscopic fields are obtained by sampling atomistic computations over parts of the computational domain; related methods have also been developed (22–31). Öttinger and coworkers (32–35) provide another example of multiscale/multilevel techniques, coupling continuum fields with stochastic evolution of molecular orientation in complex fluids (see also 36). The optimal prediction methods of Chorin and coworkers (37–39) provide a connection between microscopic/stochastic evolution and dynamics of macroscopic observables. A review (40) on extracting macroscopic dynamics [ranging from the projection operation formalism of Mori and Zwanzig (41, 42) to modern reduction methods for stochastic differential equations (e.g., 43–47)] contains a discussion of the strong relation between this approach and the coarse time-stepper we discuss below. In the adaptive mesh and algorithm refinement method (48), a direct simulation Monte Carlo is embedded at the finest level of an adaptive mesh refinement hierarchy. Many other ideas associated with the exploitation of scale separation are gradually integrated into modern multiscale computations. A strong qualitative analogy exists, for example, between approximate inertial manifolds in deterministic partial differential equations (PDEs) and the quasi-equilibrium states of Gorban, Karlin, and coworkers (49–52); use of these ideas in nonequilibrium thermodynamics can be traced back to Ehrenfest & Ehrenfest (53).

PDE: partial differential equation

The so-called heterogeneous multiscale method provides a mathematically tractable way to analyze methods of this type by first postulating an appropriate solver (what we call an outer solver) for a macroscopic equation, which is then supplemented by microscopic simulations to obtain an estimate of the unknown terms in the equation (such as the flux in a hyperbolic conservation law) (54; for a recent review, see 55). Related ideas are also mentioned by Brandt (56).

2. THE COARSE TIME-STEPPER

Let us consider an abstract fine-scale (deterministic or stochastic) evolution law and corresponding time-stepper,

$$\partial_t u(\mathbf{x}, t) = f[u(\mathbf{x}, t)], \quad u(\mathbf{x}, t + \mathrm{d}t) = s[u(\mathbf{x}, t), \mathrm{d}t], \tag{1}$$

where $u(\mathbf{x}, t)$ represents fine-scale state variables, $\mathbf{x} \in D_m$ and t are fine-scale independent variables, ∂_t denotes the time derivative, and $\mathrm{d}t$ is the fine-scale time step. We assume that a (here, deterministic) coarse model, denoted by

$$\partial_t U(\mathbf{X}, t) = F[U(\mathbf{X}, t)], \tag{2}$$

conceptually exists but is unavailable in closed form. In Equation 2, $U(\mathbf{X}, t)$ represents coarse state variables (observables), and $\mathbf{X} \in D_M$ and t are coarse independent variables. The aim is to construct a coarse time-stepper $\bar{S}$ for the variables $U(\mathbf{X}, t)$,

$$\bar{U}(\mathbf{X}, t + \delta t) = \bar{S}[\bar{U}(\mathbf{X}, t), \delta t], \tag{3}$$

where δt denotes the coarse time step, and the bars are introduced to emphasize that this is an approximation of the exact time-stepper for Equation 2 because this equation is not explicitly known.

We introduce two operators that make the transition between fine-scale and coarse variables. We define a lifting operator,

$$\mu : U(\mathbf{X}, t) \mapsto u(\mathbf{x}, t) = \mu[U(\mathbf{X}, t)], \tag{4}$$

which maps coarse to fine-scale variables, and its complement, the restriction operator,

$$\mathcal{M} : u(\mathbf{x}, t) \mapsto U(\mathbf{X}, t) = \mathcal{M}[u(\mathbf{x}, t)], \tag{5}$$

Healing: process (inherent in the simulation of the fine-scale model) that quickly restores the closure after lifting

MD: molecular dynamics

which can often be determined as soon as the coarse variables are known. For instance, when the fine-scale model evolves an ensemble of many particles, the restriction typically computes the first few moments of the distribution (density, momentum, and energy). To retain only the slow evolution on the coarse level, one could represent coarse fields using empirical basis functions (also known as Karhunen-Loève modes, proper orthogonal decomposition modes, or simply principal components) (see 57, 58). Such basis functions (modes) are extensively used in nonlinear identification and model reduction (for data compression, identification, bifurcation, and control and optimization tasks) (e.g., 59–63). Examples of equation-free computations with a proper orthogonal decomposition–mode coarse description can be found in References 64 and 65.

The construction of the lifting operator is usually much more involved. Again considering a particle model example, we need to define a mapping from a few low-order moments to initial conditions for each particle. The assumption that an equation exists that closes at the level of these low-order moments implies that higher-order moments become functionals of (or are slaved to) the low-order ones on timescales that are fast compared with the overall system evolution; in some sense, this principle also underpins quasi–steady state approximations (49, 66). Unfortunately, these slaving relations are unknown (because the coarse evolution law is also unknown). Several approaches have been suggested to address this problem. Initializing the higher-order moments randomly introduces a lifting error, and one then relies on separation of timescales to ensure that they relax quickly to functionals of the low-order moments (healing) (64, 67, 68; see also 69, 70). A detailed study of lifting errors when the microscopic model is a molecular dynamics (MD) simulation of a dense fluid can be found in Reference 71. We note that this approach may produce inaccurate results when δt is too small (72). A preparatory step, possibly involving fine-scale simulations constrained to keep the coarse observables fixed, may be required; how to accomplish this using only the fine-scale time-stepper has been explained and analyzed for singularly perturbed systems (73–76) and for lattice Boltzmann problems (77, 78).

Given an initial condition for the coarse variables $U(\mathbf{X}, t^*)$ at t^*, the coarse time-stepper (Equation 3) involves the following:

1. **Lifting.** Using the lifting operator (Equation 4), create fine-scale initial conditions $\bar{u}(\mathbf{x}, t^*)$ (Equation 1), consistent with $\bar{U}(\mathbf{X}, t^*)$.
2. **Simulation.** Use the fine-scale time-stepper (Equation 1) to compute the fine-scale state $\bar{u}(\mathbf{x}, t^*)$ at $t \in [t^*, t^* + \delta t]$.
3. **Restriction.** Obtain the coarse state $\bar{U}(\mathbf{X}, t^* + \delta t)$ from the fine-scale state $\bar{u}(\mathbf{x}, t^* + \delta t)$ using the restriction operator (Equation 5).

Assuming $\delta t = k\mathrm{d}t$, this can be written as

$$\bar{U}(\mathbf{X}, t + \delta t) = \bar{S}\,[\bar{U}(\mathbf{X}, t), \delta t] = \mathcal{M}(s^k\{\mu[\bar{U}(\mathbf{X}, t)], \mathrm{d}t\}), \tag{6}$$

where the superscript on s denotes the k fine-scale time steps. If the fine-scale model is stochastic, multiple replica simulations, using an ensemble of fine-scale initial conditions, may be needed to obtain sufficiently low-variance results.

Let us consider as a simple, illustrative example $u = (u_1, u_2)^T$ that satisfies the fine-scale equation

$$\begin{aligned} \frac{du_1}{dt} &= -u_1 - u_2 + 2, \\ \frac{du_2}{dt} &= \frac{1}{\varepsilon}\left(u_1^3 - u_2\right). \end{aligned} \tag{7}$$

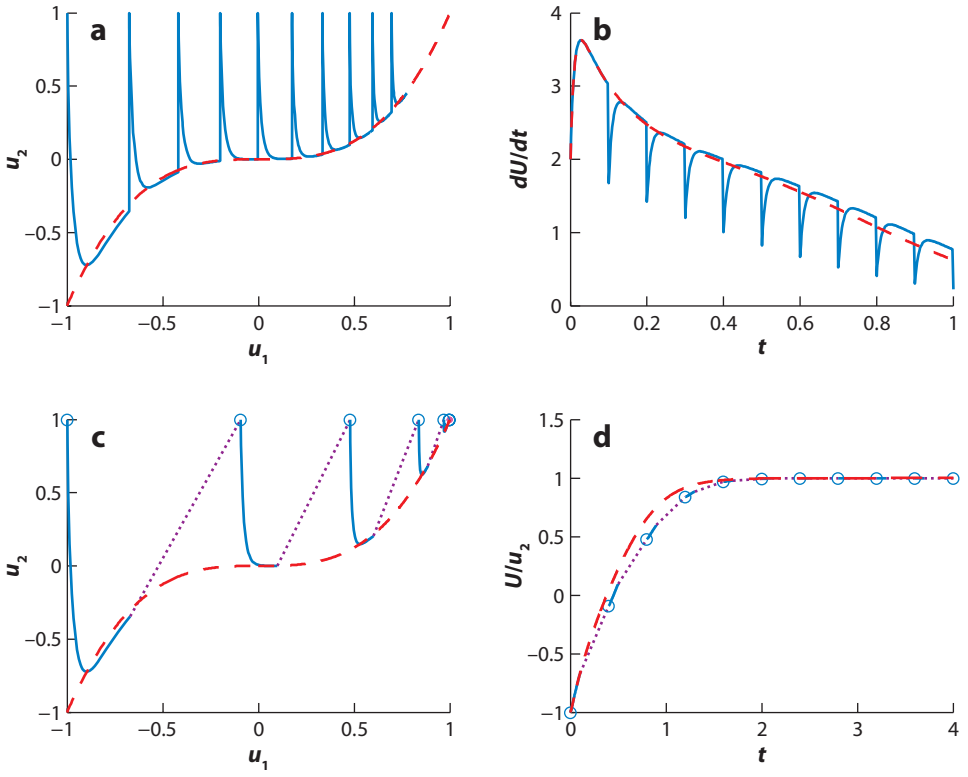

Figure 1

(*a*, *b*) Coarse time-stepper applied to Equation 7 using $\delta t = 10\varepsilon = 0.1$ and $U(0) = -1$. (*a*) The lifted solution (*blue solid line*) $u(t)$ plotted in the (u_1, u_2) phase space. At times $t = n\delta t$, the solution is restricted and then lifted again, which here amounts to setting $u_2(n\delta t) = 1$. The slow manifold is shown as a dashed red line. (*b*) The time derivative of the restricted solution $\mathcal{M}[u(n\delta t + s)]$ as a function of time $t = t$ (*blue solid line*), as well as the time derivative of the exact coarse solution $U(t) = u_1(t)$ (*red dashed line*). (*c*, *d*) Coarse projective integration. Intervals of full simulation are in blue, purple dotted lines represent projections in time, and the red dashed line is the full fine-scale simulation. (*c*) A phase space view. Whereas u_1 is projected in time corresponding to the estimated time derivative, u_2 is reset during the lifting so that the new initial condition is off the slow manifold. (*d*) The results of coarse projective integration with $\Delta t = 4\delta t$.

As the coarse variable, we consider $U = \mathcal{M}(u) = u_1$, and we define the lifting as $\mu(U) = (U, 1)^T$. **Figure 1** shows a simulation using the coarse time-stepper. The solution of Equation 7 rapidly moves to the slow manifold $u_2 = u_1^3$ for any initial data when $\varepsilon \ll 1$. The coarse time-stepper solution agrees better with the full solution (or its restriction) when ε is small or δt is large.

3. COARSE BIFURCATION ANALYSIS

Historically, the coarse time-stepper was first used to perform equation-free bifurcation computations. This was motivated by the recursive projection method (RPM) (79), a computational superstructure (wrapper) that enables the computation of bifurcation diagrams using a legacy simulation code. In the equation-free context, we consider this computational wrapper as the outer solver; the coarse time-stepper enables the computation using a fine-scale inner solver.

RPM: recursive projection method

Let us consider the coarse equation and its coarse time-stepper

$$\partial_t U = F(U, \lambda), \quad \bar{U}^{n+1} = \bar{S}(\bar{U}^n, \lambda; \Delta t), \tag{8}$$

where we have included explicit dependence on one or more parameters λ. We are interested in the asymptotic solutions (steady states, periodic orbits) of Equation 8 and their stability and dependence on λ.

A coarse steady state can be computed as a fixed point of the coarse time-stepper,

$$\bar{G}(\bar{U}, \lambda; \Delta t) = \bar{U} - \bar{S}(\bar{U}, \lambda; \Delta t) = 0. \tag{9}$$

This nonlinear system can be solved via Picard functional iterations (time-stepping until steady state is reached). However, convergence may be slow and only locates stable stationary states. Alternatively, one can solve Equation 9 using a Newton-Raphson procedure,

$$\bar{U}^{(k+1)} = \bar{U}^{(k)} + d\bar{U}^{(k)}. \tag{10}$$

Here, the correction $d\bar{U}^{(k)}$ is the solution of the linear system

$$\bar{G}_U\big(\bar{U}^{(k)}, \Delta t\big)\, \mathrm{d}\bar{U}^{(k)} = \big[I - \bar{S}_U\left(\bar{U}^{(k)}, \Delta t\right)\big]\, \mathrm{d}\bar{U}^{(k)} = -\bar{G}\big(\bar{U}^{(k)}, \Delta t\big)\,, \tag{11}$$

where $\bar{G}_U(\bar{U}^{(k)}, \Delta t)$ and $\bar{S}_U(\bar{U}^{(k)}, \Delta t)$ denote the linearization of $\bar{G}(\bar{U}, \Delta t)$ and $\bar{S}(\bar{U}, \Delta t)$, respectively, around $\bar{U}^{(k)}$, and we have again suppressed the dependence on λ for ease of notation. Because $\bar{S}_U(\bar{U}^{(k)}, \Delta t)$ is the linearization of a coarse time-stepper, we do not have its explicit formula; approximating the full Jacobian is computationally expensive.

Shroff & Keller (79) proposed RPM as a compromise between Newton-Raphson and Picard iterations, when only a legacy time-stepper is available. RPM projects the Jacobian onto the (adaptively identified, typically low-dimensional) eigenspace corresponding to the slowly varying modes. In this subspace, a Newton iteration is performed; in its orthogonal complement, Picard iterations converge fast enough. The dominant eigenvalues, and hence the stability information, are directly available as byproducts of the computation. A generalization, the Newton-Picard method, was developed to compute periodic solutions (80). These methods are efficient if the dimension of the slow (Newton) subspace is low; this condition is typically satisfied for dissipative PDEs that arise in modeling reaction and transport.

The coarse time-stepper immediately enables continuation/bifurcation computations at the coarse level, even when varying parameters of the fine-scale model, whose influence on the coarse level is difficult to assess directly. The procedure is illustrated in **Figure 2*a***. Equation-free computations using RPM have been reported in, e.g., References 16, 64, 67, 81, 83, and 84.

Let us consider a standard lattice kinetic Monte Carlo model of catalytic CO oxidation on a square lattice (67), consisting of six elementary steps:

$$\begin{aligned}
&\mathrm{CO}_{gas} + (^*)_i \rightarrow \mathrm{CO}_{ads,i},\\
&\mathrm{O}_{2,gas} + (^*)_i + (^*)_j \rightarrow \mathrm{O}_{ads,i} + \mathrm{O}_{ads,j},\\
&\mathrm{CO}_{ads,i} \rightarrow \mathrm{CO}_{gas} + (^*)_i,\\
&\mathrm{CO}_{ads,i} + \mathrm{O}_{ads,j} \rightarrow \mathrm{CO}_{2,gas} + (^*)_i + (^*)_j,\\
&\mathrm{CO}_{ads,i} + (^*)_j \rightarrow (^*)_i + \mathrm{CO}_{ads,j},\\
&\mathrm{O}_{ads,i} + (^*)_j \rightarrow (^*)_i + \mathrm{O}_{ads,j}.
\end{aligned} \tag{12}$$

Here, $(^*)_{i,j}$ represent nearest-neighbor sites on a square lattice, and lateral (repulsive or attractive) interactions between adsorbed CO are taken into account. This model can be approximated at a coarser level via two ordinary differential equations for the coverages of CO and O_2 (a mean field approximation) or by also considering fast pair probabilities (a quasichemical approximation) (67).

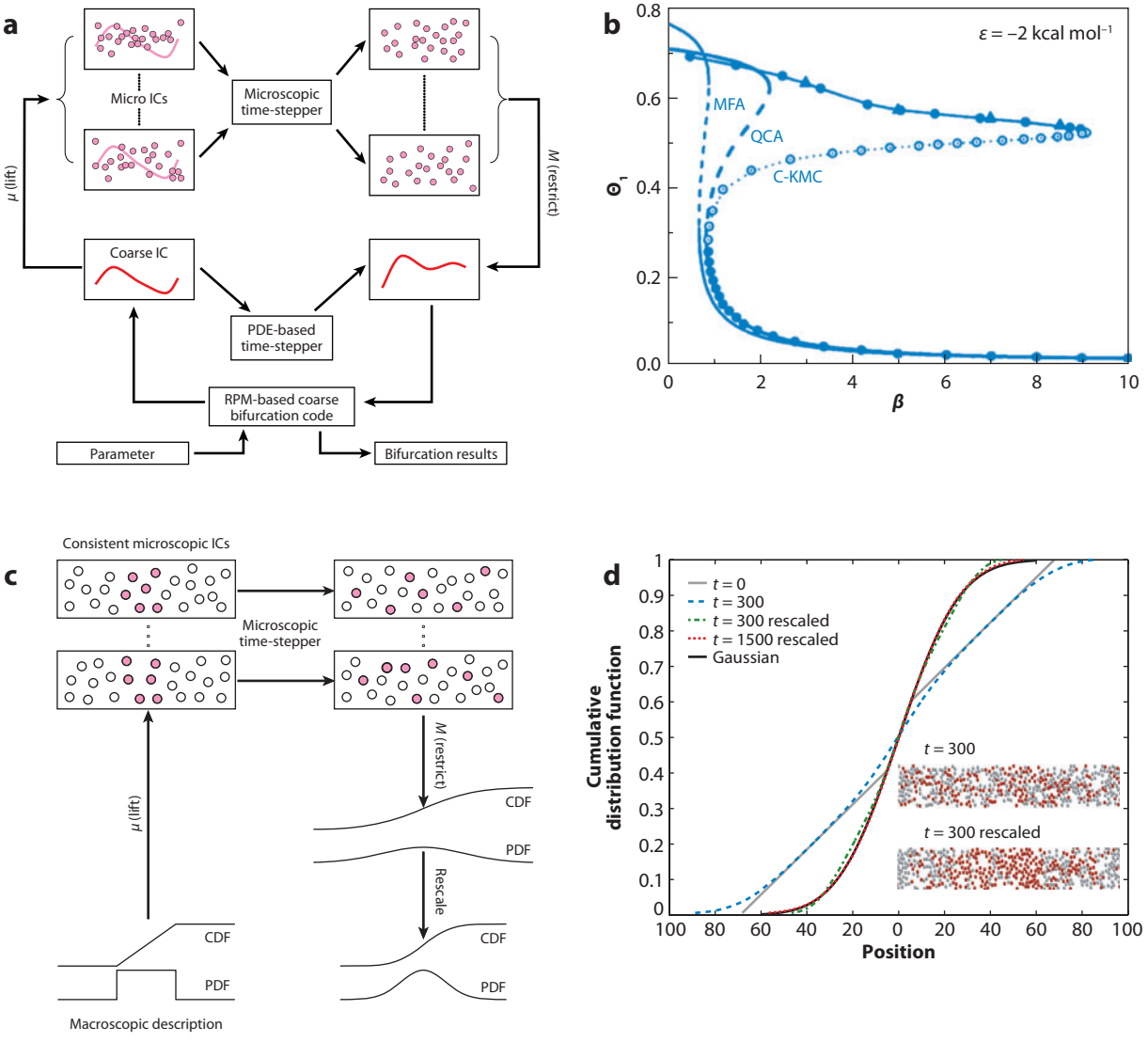

Figure 2

(*a*) Schematic of a coarse time-stepper-based bifurcation analysis. IC, initial condition; PDE, partial differential equation; RPM, recursive projection method. (*b*) Coarse bifurcation diagram (C-KMC) of the CO coverage of system (Equation 12) with respect to β (a parameter that contains the oxygen partial pressure) compared to its mean field (MFA) and quasichemical (QCA) approximations. Triangles give the long time average of full kinetic Monte Carlo simulations. Simulation details and parameters can be found in Reference 67. (*c*) Schematic view of a dynamic renormalization procedure using the coarse time-stepper. Starting with a probability density function (PDF) coarse description, through its cumulative density function (CDF), we lift to particle realizations; after fine-scale evolution, the coarse description is obtained and appropriately rescaled. (*d*) Application to the two-dimensional molecular dynamics simulation of self-diffusion, starting from a coarsely one-dimensional piecewise linear CDF. (*Inset*) A snapshot around the center of the domain at $t = 300$ (*top panel*) and the result of its restriction, rescaling, and lifting (*bottom panel*). Simulation details can be found in Reference 82.

Figure 2*b* shows a bifurcation diagram, comparing the stationary states obtained via the coarse bifurcation analysis for Equation 12 with those of the two explicit closure approximations, which clearly become inaccurate. Lifting of the coverages to individual atoms should be done in a way that correctly initializes the (implicitly slaved) pair probabilities. To this end, a preparatory fast diffusion equilibration step was performed that temporarily ignores the reactions in Equation 12 (67).

For problems with continuous symmetries, one can also compute coarse self-similar solutions, such as traveling waves/exploding solutions, as fixed points of a coarse time-stepper that incorporates an appropriate shifting/rescaling of space, time, and/or the coarse solution (see **Figure 2*c,d***). Following a template-based approach (85), one can perform a shifting/rescaling after each coarse time step; this gives the coarse time-stepper of an unavailable cotraveling/renormalized coarse evolution equation. Coarse traveling speeds/similarity exponents are a byproduct of the procedure upon convergence (82, 83, 86, 87; see also 88). An illustrative example of outer coarse self-similar diffusion dynamics based on inner MD (82) is depicted in **Figure 2*c,d***.

An alternative approach to Newton-Picard methods (which relies less on user-supplied parameters) involves solving the linear system (Equation 11) using an iterative method, such as a Krylov method. One can estimate matrix-vector products with the Jacobian as

$$\left[I - \bar{S}_U(\bar{U}, \Delta t)\right] v \approx v - \frac{\bar{S}(\bar{U} + \epsilon v, \Delta t) - \bar{S}(\bar{U}, \Delta t)}{\epsilon} \tag{13}$$

at a cost much lower than the construction of the full Jacobian. Iterative linear algebra algorithms, in their matrix-free form, are remarkably naturally suited for the equation-free framework. If required, coarse stability information can be obtained afterward, through an outer matrix-free eigensolver (89).

The convergence rate of Krylov methods (and hence the required number of matrix-vector products) depends heavily on the spectral properties of the (explicitly unavailable) system matrix in Equation 11. For rapid convergence, the eigenvalues should be clustered, for example, around one (90). Because $\bar{S}(\bar{U}, \Delta t)$ is a time-stepper, most of its eigenvalues are usually within the unit circle; the eigenvalues of $\bar{G}_U(\bar{U}, \Delta t)$ can then lie arbitrarily close to zero. Preconditioning is therefore necessary to bound the eigenvalues away from zero. We define a preconditioning matrix $M(\bar{U}, \Delta t)$ and replace the linear system (Equation 11) with

$$M\left(\bar{U}^{(k)}, \Delta t\right)^{-1} \bar{G}_U\left(\bar{U}^{(k)}, \Delta t\right) \mathrm{d}\bar{U}^{(k)} = -M\left(\bar{U}^{(k)}, \Delta t\right)^{-1} \bar{G}\left(\bar{U}^{(k)}, \Delta t\right). \tag{14}$$

Ideally, $M(\bar{U}, \Delta t)$ is a good approximation of the system matrix, for which an efficient (direct) solver is available. In the context of Jacobian-free Newton-Krylov methods, both standard preconditioning techniques, such as incomplete LU factorization and multigrid, and application-specific physics-based preconditioners have been proposed (see 91 for an overview).

In the equation-free framework, individual Jacobian elements are not available, so preconditioning techniques relying on algebraic manipulation cannot be directly applied. Several ideas have been proposed. The first is to construct a preconditioner based on a time-stepper for an approximate coarse model. A numerical convergence study with this equation-assisted idea has been performed (86), and an application to a stochastic reaction-diffusion problem was presented (92). For elliptic operators, preconditioning using different, simpler operators was originally used in References 93–95 (and references therein). An equivalent operator theory was introduced to analyze such preconditioning (96). An extension of Manteuffel & Otto's (97) analysis to the equation-free case is presented in Reference 98.

4. COARSE PROJECTIVE INTEGRATION

In this section, we review methods to accelerate the simulation of Equation 2 over large (macroscopic) time intervals. We let $\Delta t \gg \delta t$ be a large time step (commensurate with the slow coarse dynamics). In this case the outer solver is a time integrator for Equation 2 (64).

$\bar{U}^n \approx \bar{U}(n\Delta t)$ denotes the numerical approximation of the coarse solution $U(t)$, and $\bar{U}^{k,n}$ denotes the iterates of the coarse time-stepper at $t_{k,n} = n\Delta t + k\delta t$ ($\bar{U}^{0,n} \equiv \bar{U}^n$). (Here we do not lift the coarse solution at each of the k coarse time steps because a corresponding microscopic state is seamlessly available inside the coarse time-stepper.) We can then compute $\bar{U}^{n+1}$ via extrapolation, e.g.,

$$\bar{U}^{n+1} = \bar{U}^{k,n} + (\Delta t - k\delta t)\bar{F}(\bar{U}^{k,n}), \tag{15}$$

where $\bar{F}$ approximates $\bar{F}$, e.g., via finite differencing:

$$\bar{F}(\bar{U}^{k,n}) := \frac{\bar{U}^{k+1,n} - \bar{U}^{k,n}}{\delta t} \approx \frac{d\bar{U}(t_{k,n})}{dt} = \bar{F}\left[\bar{U}(t_{k,n})\right] \approx \bar{F}(\bar{U}^{k,n}). \tag{16}$$

The method in Equations 15 and 16 is called coarse projective forward Euler, and it is the simplest instantiation of this class of coarse integration methods. The procedure is illustrated for the example (Equation 7) in **Figure 1*c,d***.

The first k steps with the coarse time-stepper serve two purposes. First, they reflect that, at the fine scale, we must allow for healing of the lifting errors (those that perturb the fine-scale higher-order moments) before we can start estimating coarse time derivatives. Second, in Equation 15, extrapolation is performed starting from $\bar{U}^{k,n}$. This is particularly useful if the coarse equation contains both fast and slow modes; in that case, if the number k of inner steps is chosen large enough, one can take a large projective step, practically limited by stability restrictions on the slow modes only (99). If the extrapolation is performed starting from $\bar{U}^n$ as in the (closely related) work (100, 101), the corresponding time step is limited by the stability properties of forward Euler for the full coarse equation (for an accuracy analysis, see 102).

Higher-order versions of Equation 15 can be constructed in several ways. A straightforward idea is to use polynomial extrapolation (64). Adams-Bashforth or Runge-Kutta implementations of Equation 15 are also possible (103, 104), as are implicit versions (partially discussed in 99).

Projective integration is especially suited for problems with a large gap in their eigenvalue spectrum (see 99). A wide range of methods to obtain extended stability regions for parabolic problems [with eigenvalues along the (negative) real axis] exists (e.g., see 105, and references therein). Several extensions to projective integration methods have been presented for such cases. Telescopic projective integration (106) is a recursive version of the method: The coarse projective integrator (Equation 15) itself is now the inner integrator, around which a new projective integrator is wrapped. Another idea (based on 107) trades accuracy for stability by designing a multistep state extrapolation method using the last points of each sequence of inner steps (108).

Coarse projective integration: a class of outer algorithms that accelerate evolution of the coarse state exploiting the coarse time-stepper

Gap-tooth scheme: outer algorithm that confines fine-scale simulations to a number of small spatial subdomains of the macrodomain of interest, approximately linked through coarse interpolation

Patch dynamics: combination of coarse projective integration and gap-tooth schemes that confines fine-scale simulations to a small subset of the space-time domain (patches)

5. PATCH DYNAMICS

Coarse projective integration uses short time simulations by the fine-scale inner solver to explore long-time intervals at the coarse level. By analogy, spatially localized simulations performed in a number of small domains (teeth) separated by gaps can be appropriately linked through interpolation to enable the exploration of extended spatial systems at the coarse level (for a discussion of the resulting gap-tooth scheme, see 17, 109, 110). Here we directly proceed to describe the combination of gap-tooth with coarse integration: patch dynamics.

FD: finite difference

BC: boundary condition

For simplicity, we consider the coarse model (Equation 2) to be a PDE in one space dimension (so $\mathbf{X} = x$),

$$\partial_t U(x,t) = F\left[U(x,t), \partial_x U(x,t), \ldots, \partial_x^d U(x,t)\right], \tag{17}$$

where ∂_x^k denotes the k-th spatial derivative. Generalization to several space dimensions is straightforward. We assume the order d of Equation 17 is known; an algorithm to obtain this information using only fine-scale simulation is given in Reference 111. Given Equation 17, one can write its finite-difference (FD) method-of-lines discretization on a regular mesh as

$$\partial_t U_i(t) = F\{U_i(t), D^1[U_i(t)], \ldots, D^d[U_i(t)]\}, \quad i = 0, \ldots, N, \tag{18}$$

where $U_i(t) \approx U(x_i, t)$, $x_i \in \Pi(\Delta x) := \{0 = x_0 < x_1 = x_0 + \Delta x < \cdots < x_N = 1\}$, and $D^k[U_i(t)]$ denotes a suitable FD approximation for the k-th spatial derivative. Patch dynamics starts from an analogy with the method of lines (17). To facilitate exposition and convergence analysis, we formulate it as a time discretization of the scheme (Equation 18) (112); we can take advantage of the numerical analysis results in Reference 54 for the heterogeneous multiscale method. Discretizing in time, using forward Euler here for simplicity,

$$U^{n+1} = S(U^n; \Delta t) = U^n + \Delta t\, F(U^n), \tag{19}$$

where $U^n = [U_0(t_n), \ldots, U_N(t_n)]^T$ and Δt denotes the macroscopic time step. The dependence of $F(U^n)$ on the spatial derivatives is suppressed for notational convenience.

We define a small interval (box, tooth) of size $h \ll \Delta x$ around each (coarse) mesh point x_i and define the discrete solution $\bar{U}(t) = [\bar{U}_0(t), \ldots, \bar{U}_N(t)]^T \in \mathbb{R}^{N+1}$ as the spatially averaged restriction of the fine-scale solution in each small interval,

$$\bar{U}_i(t) = \mathcal{S}_h[\mathcal{M}(u)](x_i, t) = (1/h) \int_{x_i - h/2}^{x_i + h/2} \mathcal{M}(u)(\xi, t)\, d\xi, \quad i = 0, \ldots, N. \tag{20}$$

In higher space dimensions, these intervals become boxes around the coarse mesh points, a term that we also use here. Given an initial condition for $\bar{U}(t)$ at time t^*, a coarse time-stepper is constructed as follows:

1. **Lifting.** Use the lifting operator (Equation 4) to create initial conditions $\bar{u}_i(\mathbf{x}, t^*)$ for the microscopic model (Equation 1) in each small box around the mesh point x_i, consistent with the spatial profile of the macroscopic solution.
2. **Simulation.** Use Equation 1 to compute the microscopic state $\bar{u}_i(\mathbf{x}, t)$ in each box for $t \in [t^*, t^* + \delta t]$ employing appropriate boundary conditions (BCs).
3. **Restriction.** Obtain the spatially averaged macroscopic state $\bar{U}_i^{n+\delta}$ in each box from the microscopic state $\bar{u}_i(\mathbf{x}, t + \delta t)$ using the restriction operator (Equation 5).
4. **Projective step.** Estimate the time derivative at time t_n, e.g., as

$$\bar{F}(\bar{U}^n; h, \delta t) = \frac{\bar{U}_i^{n+\delta} - \bar{U}^n}{\delta t} \tag{21}$$

and use with a time integration method of choice, e.g., forward Euler,

$$\bar{U}^{n+1} = \bar{U}^n + \Delta t \bar{F}(\bar{U}^n; h, \delta t). \tag{22}$$

Initial conditions in each box result from a local Taylor expansion, with spatial derivatives approximated via FD on the macroscopic grid, using the (given) box averages $\bar{U}_i^n$, $i = 0, \ldots, N$,

at mesh point x_i and time t_n,

$$\bar{u}_\epsilon^i(x, t_n) = \sum_{k=0}^{2} D_i^k(\bar{U}^n)\frac{(x - x_i)^k}{k!}. \tag{23}$$

The coefficients $D_i^k(\bar{U}^n)$, $k > 0$ are the same FD approximations for the k-th spatial derivative that would be used in the method-of-lines discretization (Equation 18), whereas $D_i^0(\bar{U}^n)$ is chosen such that

$$\frac{1}{h}\int_{x_i - h/2}^{x_i + h/2} \bar{u}_\epsilon^i(\xi, t_n)\mathrm{d}\xi = \bar{U}_i^n. \tag{24}$$

Clearly, one must have information about the nature of the coarse equation; for example, if the behavior on the coarse scale is advection dominated, one should use upwind approximations for D^1. Lifting now becomes more involved because, in addition to the average value of the macroscopic unknowns in the box, we also need to initialize some approximation of the spatial derivatives of the macroscopic solution to correctly capture the dynamics of Equation 17. For noninteracting particles, one could generate initial particle positions via the inverse cumulative density function (65, 103, 113, 114). (For an MD example, we refer the reader to Reference 71.)

An additional (and crucial) difficulty is the imposition of BCs on each small box because each box is supposed to mimic local evolution of the fine-scale problem as if it were embedded in a larger domain. Indeed, patch dynamics can be thought of as a hybrid algorithm (48, 115): Each box evolves as if it were linked to a continuum description, yet this description is obtained by interpolation based on nearby boxes. Several strategies have been proposed. First, one could impose BCs that approximate the behavior of the macroscopic solution in the larger domain; for diffusion problems, based on physical considerations, one achieves this by constraining the macroscopic gradients at the box edges (17, 109). Such BCs, however, may not always be available/feasible for a given microscopic simulator; an alternative, control-based strategy has been proposed (25). Another idea is to introduce buffer regions of size H (see **Figure 3**); for a short enough simulation and large enough H, the artifacts due to essentially arbitrary BCs may

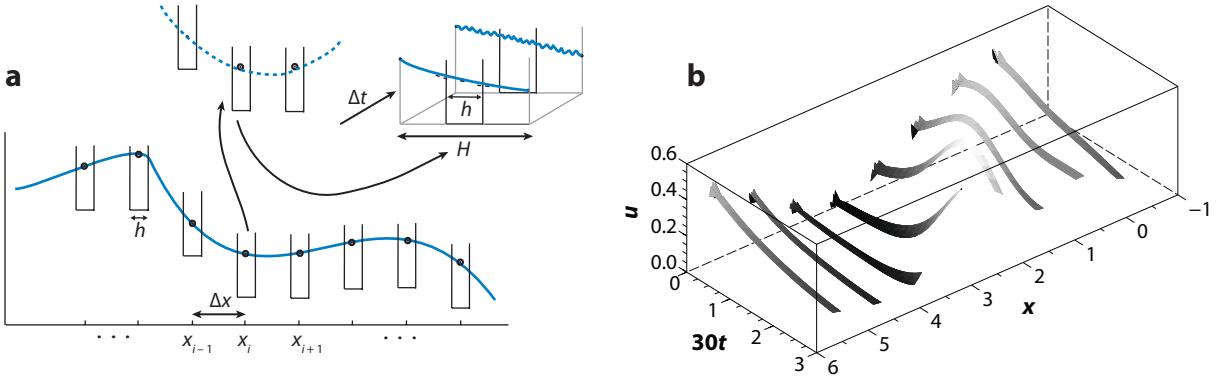

Figure 3

(*a*) Schematic representation of the gap-tooth scheme with buffer boxes. An h-sized box is chosen around each macroscopic mesh point x_i; a local Taylor approximation provides initial conditions. Simulation is performed inside the larger (buffer) boxes of size H with (arbitrary) boundary conditions (BCs). (*b*) Burgers' equation simulation using time-dependent Dirichlet BCs at teeth boundaries (for simulation details, see 110).

not affect the fine-scale simulation in the inner, h-sized region of interest. We refer readers to References 112 and 116 for a numerical analysis of patch dynamics for homogenization problems that demonstrates how H scales with δt. For diffusion problems $H = O(\sqrt{\delta t})$, and for advection-dominated problems, one needs to choose $H = O(\delta t)$. Based on holistic discretizations (117), a third proposed approach retains the possibility of imposing standard patch BCs while avoiding buffer regions (110, 118). This is achieved by updating the BCs for each patch after every fine-scale time step; the values for these BCs are obtained via center manifold theory (e.g., 119). **Figure 3*b*** shows such a gap-tooth computation of the Burgers' equation (for details, see the review in 120).

6. SELECTED APPLICATIONS

In this section, we discuss three applications in more detail. They have been selected to illustrate both the scope of the approach and the computational issues that arise in any concrete problem.

6.1. Lattice Boltzmann for Bubbly Flow

Coarse steady states of an inner lattice Boltzmann simulator for the constant speed rise of a gas bubble in a liquid (121) have been computed using an outer RPM solver (84, 122). The state space of the lattice Boltzmann model consists of a discrete set of distribution functions, corresponding to the density of particles with a given velocity (123). The coarse variables are the lowest-order moments over the velocity space (here density and momentum fields). A lifting operator distributes a given density over each of the discrete velocities with prescribed momenta; higher-order moments could be initialized randomly without crucially affecting the computations. **Figure 4** shows the coarse bifurcation diagram from linking the outer RPM solver with pseudo-arc-length continuation as the Eötvös number varies; coarse eigenvalues were obtained as a byproduct upon convergence. Notice that the coarse problem is solved without invoking surface tension—stresses in the interface region are accurately captured by the short inner lattice Boltzmann simulation itself (see 84 for simulation details and parameters).

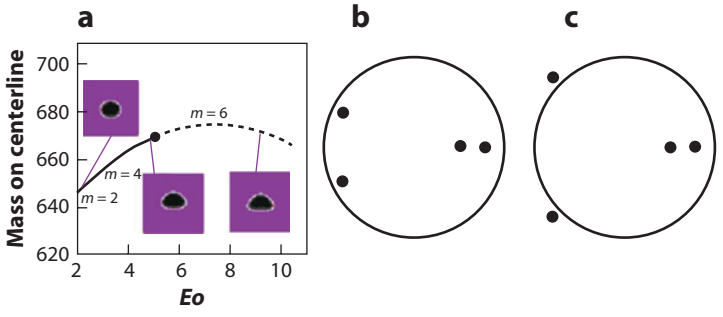

Figure 4

Coarse bifurcation diagram for a gas bubble rising in a liquid. (*a*) Total mass on the centerline versus Eötvös number. The solid line corresponds to stable steady states, whereas the dashed line represents unstable steady states. The filled circle depicts the onset of oscillations (a Hopf bifurcation). The recursive projection method parameter m represents the dimension of the slow subspace. Coarse slow eigenspectrum (*b*) just before and (*c*) after the Hopf bifurcation.

6.2. Water in Carbon Nanotubes

An MD simulation of water filling and emptying a carbon nanotube has been considered (124) (see **Figure 5*a***). Conventional MD simulations showed that, for certain values of the interaction strength λ between the carbon atoms and water, the system exhibits biphasic behavior (switching between filled and empty states on a nanosecond timescale). To study this, we constructed a coarse time-stepper over a time horizon of 1 ps for the occupancy of (the number of water molecules inside) the carbon nanotube, N. The lifting (construction of an MD initial condition with a given occupancy N) was done via a constrained MD simulation over 15 ps, in which an artificial harmonic bias potential steered the occupancy toward a target value; for variance reduction, ensemble averaging was performed over 50 replicas. When assuming effective diffusive dynamics for N, the inner simulator can be used to estimate local drift and diffusion coefficients of the corresponding Fokker-Planck equation, allowing the reconstruction of an effective free energy surface, also shown in **Figure 5*c***. Ignoring a weak dependence of the effective diffusion coefficient on N, metastable states correspond to stable fixed points of the coarse time-stepper for the chosen time step; the transition state is an unstable fixed point. **Figure 5*b*** shows a coarse bifurcation diagram of these fixed points (alternatively, of the effective free energy surface features) with respect to the interaction strength λ. Simulation details and parameter values are given in References 124–126.

GCMC: grand canonical Monte Carlo

6.3. Micelle Formation

A grand canonical Monte Carlo (GCMC) simulation of the Larson model (127) for micelle formation has been considered (128). Amphiphile and solvent molecules were modeled as a chain of beads and a single bead, respectively, and each bead occupied a site on a three-dimensional cubic lattice. The connected beads of an amphiphile were located on nearest-neighbor sites along the vectors (0,0,1), (0,1,1), and (1,1,1) and their reflections along the principal axes, resulting in a coordination number of 26. Two types of beads were considered: hydrophobic tail T and hydrophilic head H. The solvent beads were taken to be equal to the head beads. Details of the interactions among the beads, system, and simulation parameters can be found in Reference 128. A representative snapshot of a simulation is shown in **Figure 6*a***.

As micelles formed and broke in the simulation, the physical properties of a cluster, such as its radii of gyration and energy, appeared to quickly become slaved to the cluster size; it was therefore assumed (and numerically verified) that cluster size ψ was a good coarse variable (129). The lifting operator (which maps coarse states ψ to GCMC realizations) used a database of cluster structures kept from long simulation. This system exhibited diffusive dynamics in ψ (129), again allowing the approximation—using the inner simulator—of an effective free energy surface from the corresponding Fokker-Planck equation (see **Figure 6*b***). The free energy barrier, which corresponds to an unstable fixed point of the coarse time-stepper, was located using coarse reverse projective integration (**Figure 6*c***) (see also 103). This again assumed weak state dependence of the effective diffusion coefficient (see **Figure 6*b***). Forward simulation using the inner GCMC code and restriction to ψ were followed by a large backward projective step, along the locally estimated drift of the effective Fokker-Planck equation, moving up the effective free energy surface. Owing to its peculiar stability properties, reverse projective integration can locate unstable steady states with fast decaying stable modes and slowly growing unstable ones (130). The coarse variable ψ becomes less successful in describing dynamics when it takes low values; **Figure 6*d*** suggests that a second coarse variable (such as a cluster energy density) may be required there.

Figure 5

(*a*) Schematic of the carbon nanotube (CNT)-water system as a cylinder surrounded by water molecules, showing vestibules at the cylinder ends, introduced to allow smooth variation in the occupancy. (*b*) Coarse bifurcation diagram. Solid filled squares correspond to (stable) fully filled ($N > 5$) or empty ($N < 1$) states. Open circles correspond to (unstable) partially filled states. The turning points are indicated with filled diamonds. A number of representative structures are shown along the dashed vertical lines. (*Inset*) The effective bifurcation diagram obtained through histogram reweighting. (*c*) The effective free energy surfaces corresponding to the dashed vertical lines in panel *b*.

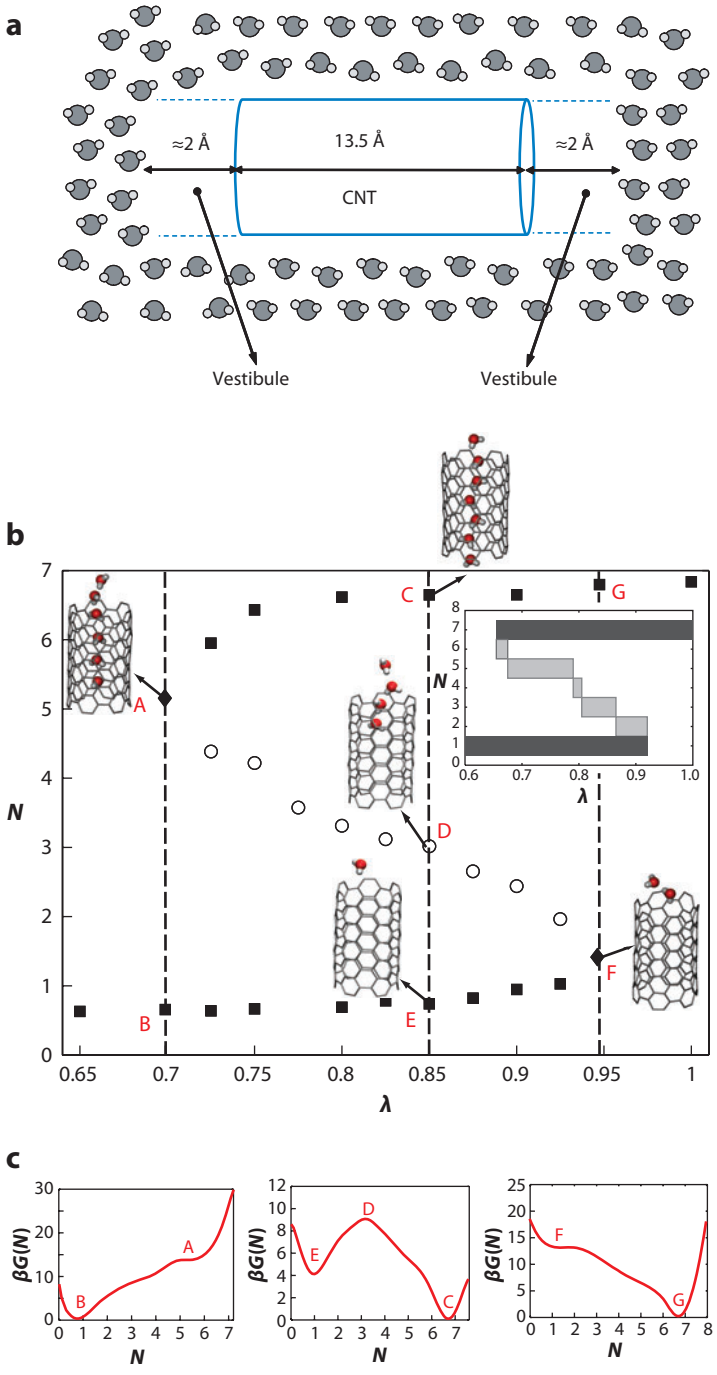

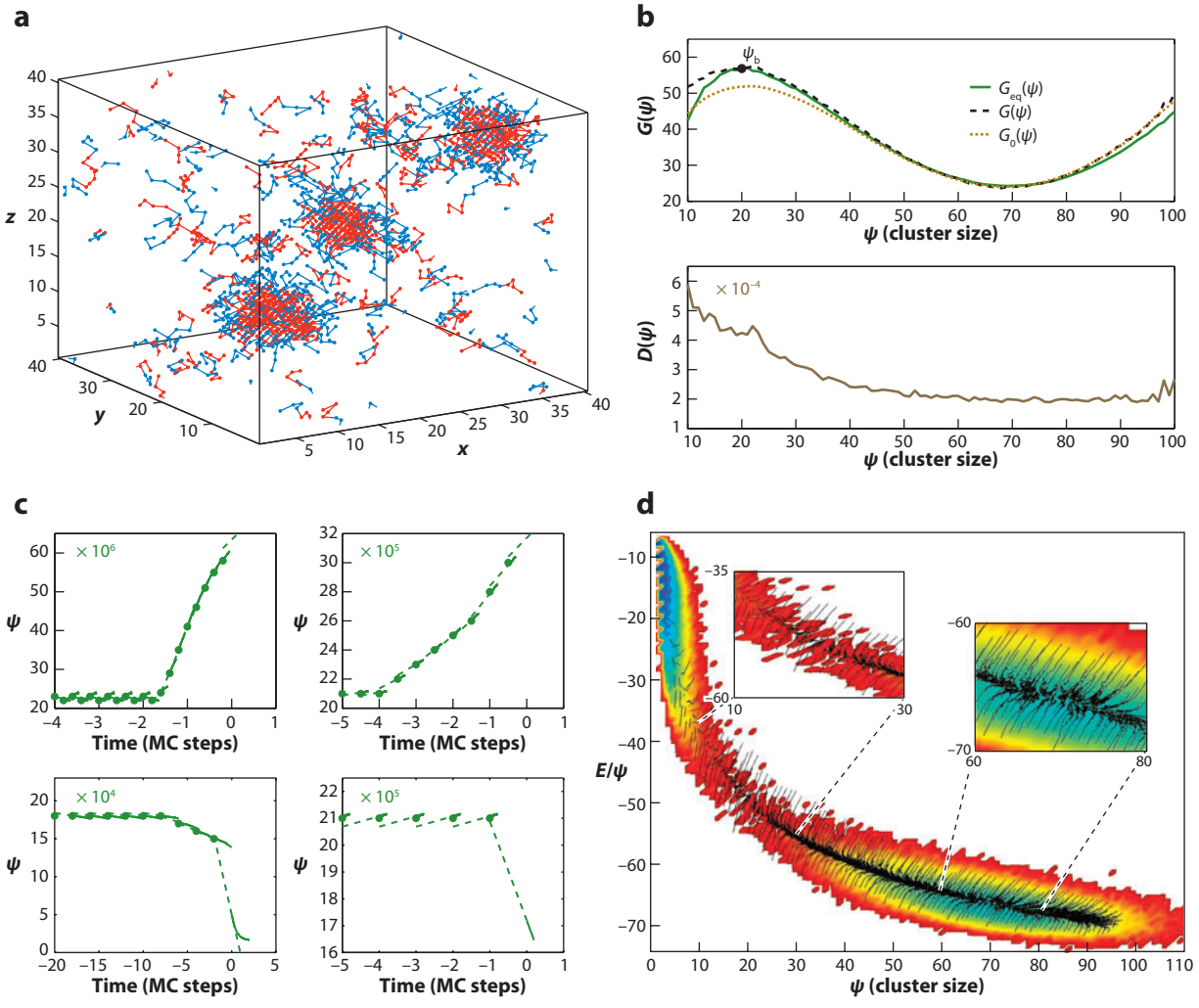

Figure 6

(*a*) Snapshot of a micelle-forming system. Hydrophobic tail beads are shown in red, and hydrophilic head beads are shown in blue (solvent beads are not shown). (*b*) Free energy surface obtained from equilibrium simulations (*solid green line*), a kinetic approach (*dashed black line*), and an approximation that neglects the weak spatial dependence of the diffusion coefficients depicted below. (*c*) Coarse reverse projective integration starting at different initial values and for different method parameters. The restrictions of the short forward simulations are represented by the solid line, and the backward coarse projections are represented by the dashed line. MC, Monte Carlo. (*d*) A two-dimensional effective free energy surface, suggesting the need for additional coarse variables at low cluster sizes. Simulation details can be found in References 128 and 129.

7. CONCLUSIONS AND OUTLOOK

Above we review an equation-free framework for modeling and computation in complex/multiscale systems that bypasses the derivation of macroscopic evolution equations when these equations conceptually exist but are not available in closed form. Established continuum numerical algorithms motivate the construction of computational wrappers around fine-scale simulators via a lift-run-restrict procedure that enables the performance of system-level tasks (such as bifurcation and

stability analysis, control, optimization, and even accelerated simulation over extended spatio-temporal domains). Ultimately, the framework is an input-output one: Information traditionally obtained by evaluating a coarse-level model is extracted on demand from short bursts of appropriately initialized simulations with the fine-scale code. Significant progress has been made over the past years in developing and analyzing projective and patch dynamics schemes and exploiting the properties of the coarse time-stepper to perform system-level tasks (efficient numerical bifurcation analysis, coarse dynamic renormalization).

Applications of this framework are diverse: nematic liquid crystal rheology (68), heterogeneous population dynamics (131, 132), agent-based models and network dynamics (133, 134), bacterial chemotaxis (114), neural oscillator activity (135), stellar cluster collapse (136), stochastic dynamics of gene regulatory networks (137), structural transitions in crystals (138), optimization and control (68, 139), and more.

Clearly, when accurate explicit equations exist, they should be used. In their absence, when equation-free computations become necessary, approximate closed equations can still increase efficiency as preconditioners—in equation-assisted computations. When some degree of analytical coarse graining can be achieved, equation-free algorithms can be wrapped around this coarsest accurate model, hopefully enhancing its scope. As our GCMC example illustrates, the inner simulator does not need to model physical time evolution: Dynamics representing, for instance, sampling of an equilibrium distribution may also be accelerated.

Although significant progress has been made, several issues require further attention. For instance, although the effects of the lifting operator on the accuracy and efficiency of the methods are understood for simple model problems (e.g., 75–77), the development of efficient and systematic algorithms for initializing fine-scale simulations conditioned on coarse states continues to be a truly challenging area of research.

When experience or physical intuition is insufficient for the detection of appropriate coarse variables, one appeals to modern data-mining/manifold learning techniques, such as Isomap (140) or diffusion maps (141–144) (see 137 for an example of variable-free equation-free computations using a diffusion map approach, with the coarse variables themselves also obtained from fine-scale simulation). Combining the detection of the right variables with the ability to perform differential operations on them forms the basis for a type of calculus of complex systems.

Noise and its treatment are ubiquitous in the formulation and the analysis of the framework we discuss above, from the robustness of traditional algorithms (145) and the variance-reduced local estimation of quantities for coarse numerical computation (34) to the identification of effective stochastic models (40, 146) and hypothesis testing for the closure level or the nature of the unavailable equations (111). This review does not do justice to these important issues, on which we also expect extensive future research.

We conclude with two directions in which this approach may have significant impact. The first is the quantitative exploration of individual-based models in socioeconomic sciences; here, tools from statistical mechanics are already making a difference (e.g., 147), and we expect multiscale methods, such as the ones described above, to enhance this trend. The second area involves equation-free laboratory experimentation. Today one can increasingly find experimental systems in which enough control/actuation authority exists for initial/boundary conditions to be easily physically implemented [e.g., the construction of configurations of colloidal particles with prescribed statistics using optical tweezers (148)]. In such systems, equation-free computational protocols in principle can translate to laboratory experimental design; optimization protocols (from traditional response surface approaches to genetic algorithms) are increasingly used experimentally in recent years (e.g., 149, 150). Recursive design of sequences of short experiments may allow the laboratory implementation of many numerical

algorithms currently used only on computer models—a dream of doing mathematics directly on nature.

SUMMARY POINTS

1. Many complex physical/engineering problems are modeled at space and time scales drastically finer than the (macroscopic, coarse) level at which experimental observations are typically made and at which practical tasks such as prediction, design, and optimization need to be performed. Full simulation with these fine-scale models cannot hope to address such practical tasks. Traditionally, closures are obtained (through experiment and observation or through rigorous mathematics) to formulate useful models at the coarse level directly.
2. We present an approach that circumvents the explicit derivation of such closures and macroscopic models. The closure is obtained on demand through brief simulation of the fine-scale model over relatively short space and time scales. The approach is a design of (computational) experiments, using the fine-scale model as an experiment that can be initialized, executed, and observed at will.
3. In this framework, traditional numerical algorithms, from initial value solvers and spatial discretization techniques to contraction mappings and (especially) iterative matrix-free linear algebra, dictate the construction of computational wrappers: outer algorithms that perform coarse modeling tasks by designing, executing, and processing the results of computational experiments with an inner fine-scale solver.
4. Lifting operators that create fine-scale states consistent with coarse observations (a one-to-many procedure) and restriction operators that (conversely) coarsely observe fine-scale states are crucial elements of the framework. They correspond to initializing an experiment and observing/taking measurements from it. As our selected applications show, systematic lifting can be a computationally intensive process, for which problem-specific insight is often invaluable.
5. The scope of the framework (in terms of the type of outer solvers developed, the nature of the inner solvers, and the possible applications) is broad, as illustrated in our selected applications. It naturally brings together and functionally integrates elements of fine-scale/atomistic simulation, continuum numerical analysis, identification and control, statistics, and hypothesis testing.

FUTURE ISSUES

1. Before the unavailable equation is solved, we need to be able to answer certain qualitative questions that crucially affect the algorithms and that are much easier to answer with closed-form models: What is the correct level at which a model can usefully close? Is the unavailable equation a PDE (of what order?), a stochastic PDE, or an integral equation? Is it Hamiltonian or a conservation law? Does it exhibit space or scale symmetry? Tools for answering these questions based on fine-scale simulation results should be systematically developed.

2. What are the right variables in terms of which the macroscopic model can be written? For many problems, they are known by experience and long experimentation, physical intuition, or rigorous mathematical derivation. Yet there is an increasing need to automatically extract such variables from available observations and to even design experimentation (possibly computational) for data acquisition with this purpose in mind. The link to modern data-mining/manifold learning techniques is a crucial one, and lifting/restriction based on such variables should be systematically studied.
3. Error analysis for the type of algorithms we describe (including a posteriori estimates) is at its infancy, especially for atomistic inner solvers. Issues of automatic adaptive refinement in space and time, adaptively controlled variance reduction of noise (linking to modern data-estimation techniques), and on-the-fly verification of the level of closure all are important research subjects. Numerical analysts are already studying several aspects (e.g., see the work of W.E, B. Engquist, and coworkers).
4. We believe this type of work may have a transformative impact on the individual-based modeling of social/economic phenomena, enabling a higher level of quantitative study.
5. We envision that, for physical systems in which enough spatiotemporally resolved sensing and actuation authority exists to initialize at will, the wrapper algorithms (computational experiment design protocols) we discuss may become laboratory experimental design protocols. One day, one might be able to perform computer-assisted mathematical tasks directly on nature through the same algorithms used today to perform these tasks on models.

DISCLOSURE STATEMENT

The authors are not aware of any biases that might be perceived as affecting the objectivity of this review.

ACKNOWLEDGMENTS

Starting with the first paper (16) of this program, the original inspiration of the work of H. Keller (1925–2008) is clear; he taught us a lot, and we are poorer without him. Over the years, there have been many exciting and fruitful collaborations with many scientists—friends, colleagues, students, and postdocs. We would greatly exceed our space limitations to do justice to them and apologize for this while acknowledging what pleasure and honor these collaborations have been. I.G.K. feels he should mention C.W. Gear, G. Hummer, C. Siettos, and R. Coifman among them. G.S. has been supported by the Research Foundation Flanders (FWO-Vlaanderen) as a Research Assistant and then Postdoctoral Fellow throughout our collaboration. The research of I.G.K. was initially supported by AFOSR; subsequent support from DARPA, NSF, ACS/PRF, and the U.S. DOE is also gratefully acknowledged.

LITERATURE CITED

1. Bensoussan A, Lions JL, Papanicolaou G. 1978. *Studies in Mathematics and its Applications*, Vol. 5: *Asymptotic Analysis of Periodic Structures*. Amsterdam: North-Holland
2. Bornemann F. 1998. *Homogenization in Time of Singularly Perturbed Mechanical Systems*. Berlin: Springer
3. Goldenfeld N. 1992. *Lectures on Phase Transitions and the Renormalization Group*. Reading, MA: Perseus

4. Constantin P, Foias C, Nicolaenko B, Temam R. 1988. *Integral Manifolds and Inertial Manifolds for Dissipative Partial Differential Equations*. New York: Springer
5. Katsoulakis M, Majda A, Vlachos D. 2003. Coarse-grained stochastic processes and Monte Carlo simulations in lattice systems. *J. Comput. Phys.* 186:250–78
6. Balescu R. 1975. *Equilibrium and Nonequilibrium Statistical Mechanics*. New York: Wiley & Sons
7. Gaspard P. 1998. *Chaos, Scattering and Statistical Mechanics*. Cambridge: Cambridge Univ. Press
8. Chapman S, Cowling TG. 1991. *The Mathematical Theory of Non-Uniform Gases: An Account of the Kinetic Theory of Viscosity, Thermal Conduction and Diffusion in Gases*. Cambridge: Cambridge Univ. Press
9. Vincenti WG, Kruger CH. 1965. *Introduction to Physical Gas Dynamics*. New York: Wiley
10. Boon JP, Yip S. 1980. *Molecular Hydrodynamics*. New York: McGraw-Hill
11. Van Kampen NG. 2007. *Stochastic Processes in Physics and Chemistry*. Amsterdam: North-Holland
12. Spohn H. 1991. *Large Scale Dynamics of Interacting Particles*. New York: Springer-Verlag
13. Keunings R. 2004. Micro-macro methods for the multiscale simulation of viscoelastic flows using molecular methods of kinetic theory. In *Rheology Reviews*, ed. DM Binding, K Walters, pp. 67–98. Aberystwyth, UK: Brit. Soc. Rheol.
14. Erban R, Othmer HG. 2004. From individual to collective behavior in bacterial chemotaxis. *SIAM J. Appl. Math.* 65:361–91
15. Attinger S. 2003. Generalized coarse-graining procedures for flow in porous media. *Comput. Geosci.* 7:253–73
16. **Theodoropoulos C, Qian YH, Kevrekidis IG. 2000. Coarse stability and bifurcation analysis using time-steppers: a reaction-diffusion example. *Proc. Natl. Acad. Sci. USA* 97:9840–45**
17. **Kevrekidis IG, Gear CW, Hyman JM, Kevrekidis PG, Runborg O, Theodoropoulos C. 2003. Equation-free, coarse-grained multiscale computation: enabling microscopic simulators to perform system-level tasks. *Comm. Math. Sci.* 1:715–62**
18. Kelley CT. 1995. *Iterative Methods for Linear and Nonlinear Equations*. Philadelphia: SIAM
19. Phillips R. 2001. *Crystals, Defects and Microstructures: Modeling Across Scales*. Cambridge: Cambridge Univ. Press
20. Shenoy VB, Miller R, Tadmor E, Rodney D, Phillips R, Ortiz M. 1999. An adaptive finite element approach to atomic-scale mechanics: the quasicontinuum method. *J. Mech. Phys. Solids* 47:611–42
21. Ortiz M, Phillips R. 1999. Nanomechanics of defects in solids. *Adv. Appl. Mech.* 36:1–79
22. Xu K, Prendergast KH. 1994. Numerical Navier-Stokes solutions from gas-kinetic theory. *J. Comput. Phys.* 114:9–17
23. Bulatov V, Abraham FF, Kubin L, Devincre B, Yip S. 1998. Connecting atomistic and mesoscale simulations of crystal plasticity. *Nature* 391:669–72
24. Li J, Liao D, Yip S. 1998. Imposing field boundary conditions in MD simulation of fluids: optimal particle controller and buffer zone feedback. *Mater. Res. Soc. Symp. Proc.* 538:473–78
25. Li J, Liao D, Yip S. 1998. Coupling continuum to molecular-dynamics simulation: reflecting particle method and the field estimator. *Phys. Rev. E* 57:7259–67
26. Abraham FF, Bernstein N, Broughton JQ, Hess D. 2000. Dynamic fracture of silicon: concurrent simulation of quantum electrons, classical atoms, and the continuum solid. *Mater. Res. Soc. Bull.* 25(5):27–32
27. Abraham FF, Broughton JQ, Bernstein N, Kaxiras E. 1998. Spanning the length scales in dynamic simulation. *Comput. Phys.* 12:538–46
28. Xu K. 2001. A gas-kinetic BGK scheme for the Navier-Stokes equations and its connection with artificial dissipation and Godunov method. *J. Comput. Phys.* 171:289–335
29. Smith GS, Tadmor EB, Bernstein N, Kaxiras E. 2001. Multiscale simulations of silicon nanoindentation. *Acta Mater.* 49:4089–101
30. Curtin WA, Miller RE. 2003. Atomistic/continuum coupling in computational materials science. *Model. Simul. Mater. Sci. Eng.* 11:R33–68
31. Tammaro M, Sabella M, Evans JW. 1995. Hybrid treatment of spatio-temporal behavior in surface reactions with coexisting immobile and highly mobile reactants. *J. Chem. Phys.* 103:10277–85
32. Öttinger HC. 1996. *Stochastic Processes in Polymeric Fluids*. Berlin: Springer
33. Laso M, Öttinger HC. 1993. Calculation of viscoelastic flow using molecular models: the CONNFFESSIT approach. *J. Non-Newton. Fluid Mech.* 47:1–20

16. First published equation-free computations using a coarse time-stepper for an inner lattice-Boltzmann solver through an outer RPM wrapper.

17. First extensive review of equation-free methods, with detailed discussion of principles, algorithms, applications, and possibilities.

34. Öttinger HC, van den Brule BHAA, Hulsen MA. 1997. Brownian configuration fields and variance reduced CONNFESSIT. *J. Non-Newton. Fluid Mech.* 70:255–61
35. Hulsen MA, van Heel APG, van den Brule BHAA. 1997. Simulation of viscoelastic flows using Brownian configuration fields. *J. Non-Newton. Fluid Mech.* 70:79–101
36. Jendrejack RM, de Pablo JJ, Graham MD. 2002. A method for multiscale simulation of flowing complex fluids. *J. Non-Newton. Fluid Mech.* 108:123–42
37. Chorin AJ, Hald OH, Kupferman R. 2000. Optimal prediction and the Mori-Zwanzig representation of irreversible processes. *Proc. Natl. Acad. Sci. USA* 97:2968–73
38. Chorin AJ, Kast AP, Kupferman R. 1998. Optimal prediction of underresolved dynamics. *Proc. Natl. Acad. Sci. USA* 95:4094–98
39. Chorin AJ, Hald OH, Kupferman R. 2002. Optimal prediction with memory. *Phys. D Nonlinear Phenom.* 166:239–57
40. Givon D, Kupferman R, Stuart A. 2004. Extracting macroscopic dynamics: model problems and algorithms. *Nonlinearity* 17:R55–127
41. Mori H. 1965. Transport, collective motion and Brownian motion. *Prog. Theor. Phys.* 33:423–50
42. Zwanzig R. 1973. Nonlinear generalized Langevin equations. *J. Stat. Phys.* 9:215–20
43. Majda AJ, Timofeyev I, Vanden-Eijnden E. 2001. A mathematical framework for stochastic climate models. *Commun. Pure Appl. Math.* 54:891–947
44. Huisinga W, Schutte C, Stuart AM. 2003. Extracting macroscopic stochastic dynamics: model problems. *Commun. Pure Appl. Math.* 56:234–69
45. Shardlow T, Stuart AM. 2000. A perturbation theory or ergodic Markov chains and application to numerical approximations. *SIAM J. Numer. Anal.* 37:1120–37
46. Vanden-Eijnden E. 2003. Numerical techniques for multiscale dynamical systems with stochastic effects. *Commun. Math. Sci.* 1:377–84
47. E W, Liu D, Vanden-Eijnden E. 2005. Analysis of numerical techniques for multiscale stochastic dynamical systems. *Commun. Pure Appl. Math.* 58:1544–85
48. Garcia AL, Bell JB, Crutchfield WY, Alder BJ. 1999. Adaptive mesh and algorithm refinement using direct simulation Monte Carlo. *J. Comput. Phys.* 154:134–55
49. Gorban AN, Karlin IV. 2005. *Invariant Manifolds for Physical and Chemical Kinetics*. Berlin: Springer-Verlag
50. Gorban AN, Karlin IV. 2002. Macroscopic dynamics through coarse-graining: a solvable example. *Phys. Rev. E* 65:026116
51. Gorban AN, Karlin IV, Ilg P, Öttinger HC. 2001. Corrections and enhancements of quasi-equilibrium states. *J. Non-Newton. Fluid Mech.* 96:203–19
52. Gorban AN, Karlin IV, Öttinger HC, Tatarinova LL. 2001. Ehrenfest's argument extended to a formalism of nonequilibrium thermodynamics. *Phys. Rev. E* 63:066124
53. Ehrenfest P, Ehrenfest T. 1959 (1911). *The Conceptual Foundations of the Statistical Approach in Mechanics*. Transl. MJ Moravcsik. Ithaca, NY: Cornell Univ. Press
54. E W, Engquist B. 2003. The heterogeneous multiscale methods. *Commun. Math. Sci.* 1:87–132
55. E W, Engquist B, Li X, Ren W, Vanden-Eijnden E. 2007. Heterogeneous multiscale methods: a review. *Commun. Comput. Phys.* 2:367–450
56. Brandt A. 2002. Multiscale scientific computation: review 2001. In *Multiscale and Multiresolution Methods: Theory and Applications*, ed. TJ Barth, T Chan, R Haimes, pp. 3–96. Berlin: Springer-Verlag
57. Holmes P, Lumley J, Berkooz G. 1996. *Turbulence, Coherent Structures, Dynamical Systems and Symmetry*. Cambridge: Cambridge Univ. Press
58. Sirovich L, Rodriguez J. 1987. Coherent structures and chaos: a model problem. *Phys. Lett. A* 120:211–14
59. Shvartsman S, Kevrekidis IG. 1998. Nonlinear model reduction for control distributed systems: a computer-assisted study. *AIChE J.* 44:1579–95
60. Yeşilyurt S, Patera A. 1995. Surrogates for numerical simulations: optimization of eddy-promoter heat exchangers. *Comput. Methods Appl. Mech. Eng.* 121:231–57
61. Rico-Martinez R, Kevrekidis IG, Titi E. 2000. Order reduction for nonlinear dynamic models of distributed reacting systems. *J. Process Control* 10:177–84

40. Extensive review, giving a detailed discussion of many analytical and numerical multiscale approaches, with ample references.

62. Deane AE, Kevrekidis IG, Karniadakis GE, Orszag SA. 1991. Low-dimensional models for complex geometry flows: application to grooved channels and circular cylinders. *Phys. Fluids A* 3:2337–54
63. Aubry N, Holmes P, Lumley J, Stone E. 1988. The dynamics of coherent structures in the wall region of a turbulent boundary layer. *J. Fluid Mech.* 192:115–73
64. Gear CW, Kevrekidis IG, Theodoropoulos C. 2002. Coarse integration/bifurcation analysis via microscopic simulators: micro-Galerkin methods. *Comput. Chem. Eng.* 26:941–63
65. Setayeshar S, Gear CW, Othmer HG, Kevrekidis IG. 2005. Application of coarse integration to bacterial chemotaxis. *SIAM Multiscale Model. Simul.* 4:307–27
66. Bodenstein M. 1913. Eine Theorie der photochemischen Reaktionsgeschwindigkeiten. *Z. Phys. Chem.* 85:329–97
67. Makeev AG, Maroudas D, Panagiotopoulos AZ, Kevrekidis IG. 2002. Coarse bifurcation analysis of kinetic Monte Carlo simulations: a lattice-gas model with lateral interactions. *J. Chem. Phys.* 117:8229–40
68. Siettos CI, Graham MD, Kevrekidis IG. 2003. Coarse Brownian dynamics for nematic liquid crystals: bifurcation, projective integration and control via stochastic simulation. *J. Chem. Phys.* 118:10149–57
69. Ryckaert JP, Ciccotti G, Berendsen H. 1977. Numerical integration of the Cartesian equation of motion of a system with constraints: molecular dynamics of *n*-alkanes. *J. Comp. Phys.* 23:327–41
70. Torrie GM, Valleau JP. 1974. Monte Carlo free energy estimation using non-Boltzmann sampling: application to the subcritical Lennard Jones fluid. *Chem. Phys. Lett.* 28:578–81
71. Frederix Y, Samaey G, Vandekerckhove C, Li T, Nies E, Roose D. 2008. Lifting in equation-free methods for molecular dynamics simulations of dense fluids. *Discret. Contin. Dyn. Syst. Ser. B.* In press
72. Van Leemput P, Lust K, Kevrekidis IG. 2005. Coarse-grained numerical bifurcation analysis of lattice Boltzmann models. *Phys. D Nonlinear Phenom.* 210:58–76
73. Gear CW, Kaper TJ, Kevrekidis IG, Zagaris A. 2005. Projecting to a slow manifold: singularly perturbed systems and legacy codes. *SIAM J. Appl. Dyn. Syst.* 4:711–32
74. Gear CW, Kevrekidis IG. 2005. Constraint-defined manifolds: a legacy code approach to low-dimensional computation. *J. Sci. Comput.* 25:17–28
75. Zagaris A, Gear CW, Kaper T, Kevrekidis IG. 2008. Analysis of the accuracy and convergence of equation-free projection to a slow manifold. *Math. Mod. Numer. Anal.* In press
76. Zagaris A, Vandekerckhove C, Gear CW, Kaper T, Kevrekidis IG. 2008. Stability and stabilization of the constrained runs schemes for equation-free projection to a slow manifold. Submitted manuscript
77. Van Leemput P, Vanroose W, Roose D. 2007. Mesoscale analysis of the equation-free constrained runs initialization scheme. *Multiscale Model. Simul.* 6:1234–55
78. Vandekerckhove C, Roose D, Kevrekidis IG. 2008. An efficient Newton-Krylov implementation of the constrained runs scheme for initializing on a slow manifold. *J. Sci. Comput.* In press
79. Shroff GM, Keller HB. 1993. Stabilization of unstable procedures: the recursive projection method. *SIAM J. Numer. Anal.* 30:1099–120
80. Lust K, Roose D, Spence A, Champneys AR. 1998. An adaptive Newton-Picard algorithm with subspace iteration for computing periodic solutions. *SIAM J. Sci. Comput.* 19:1188–209
81. Makeev AG, Maroudas D, Kevrekidis IG. 2002. Coarse stability and bifurcation analysis using stochastic simulators: kinetic Monte Carlo examples. *J. Chem. Phys.* 116:10083–91
82. Chen L, Debenedetti P, Gear CW, Kevrekidis IG. 2004. From molecular dynamics to coarse self-similar solutions: a simple example using equation-free computation. *J. Non-Newton. Fluid Mech.* 120:215–23
83. Runborg O, Theodoropoulos C, Kevrekidis IG. 2002. Effective bifurcation analysis: a time-stepper based approach. *Nonlinearity* 15:491–511
84. Theodoropoulos C, Sankaranarayanan K, Sundaresan S, Kevrekidis IG. 2004. Coarse bifurcation studies of bubble flow lattice Boltzmann simulations. *Chem. Eng. Sci.* 59:2357–62
85. Rowley C, Marsden J. 2000. Reconstruction equations and the Karhunen-Loève expansion for systems with symmetry. *Phys. D Nonlinear Phenom.* 142:1–19
86. Samaey G, Vanroose W, Roose D, Kevrekidis IG. 2008. Newton-Krylov solvers for the equation-free computation of coarse traveling waves. *Comput. Methods Appl. Mech. Eng.* 197:3480–91
87. Kavousanakis ME, Erban R, Boudouvis AG, Gear CW, Kevrekidis IG. 2007. Projective and coarse projective integration for problems with continuous symmetries. *J. Comput. Phys.* 225:382–407

73. Analysis of a lifting algorithm that constructs an appropriate fine-scale state from a coarse state, given only a fine-scale simulator.

79. Describes a computational superstructure wrapped around a legacy time-stepper to directly compute steady states.

88. Chen L, Goldenfeld N. 1995. Numerical renormalization-group calculations for similarity solutions and traveling waves. *Phys. Rev. E* 51:5577–81
89. Lehoucq RB, Salinger AG. 2001. Large-scale eigenvalue calculations for stability analysis of steady flows on massively parallel computers. *Int. J. Numer. Methods Fluids* 36:309–27
90. Saad Y. 2003. *Iterative Methods for Sparse Linear Systems*. Philadelphia: SIAM
91. Knoll DA, Keyes DE. 2004. Jacobian-free Newton-Krylov methods: a survey of approaches and applications. *J. Comput. Phys.* 193:357–97
92. Qiao L, Erban R, Kelley CT, Kevrekidis IG. 2006. Spatially distributed stochastic systems: equation-free and equation-assisted bifurcation analysis. *J. Chem. Phys.* 125:204108
93. D'Yakanov EG. 1961. On an iterative method for the solution of a system of finite-difference equations. *Dokl. Akad. Nauk* 138:522–25
94. Gunn JE. 1964. The solution of elliptic difference equations by semiexplicit iterative techniques. *Numer. Math.* 6:181–84
95. Axelsson O, Karátson J. 2004. Superlinearly convergent CG methods via equivalent preconditioning for nonsymmetric elliptic operators. *Numer. Math.* 99:197–223
96. Faber V, Manteuffel T, Parter S. 1990. On the theory of equivalent operators and application to the numerical solution of uniformly elliptic partial-differential equations. *Adv. Appl. Math.* 11:109–63
97. Manteuffel T, Otto J. 1993. Optimal equivalent preconditioners. *SIAM J. Numer. Anal.* 30:790–812
98. Samaey G, Vanroose W, Kevrekidis IG. 2008. Equivalent operator preconditioning of equation-free Newton-Krylov computations. *SIAM J. Numer. Anal.* Manuscript submitted
99. Gear CW, Kevrekidis IG. 2003. Projective methods for stiff differential equations: problems with gaps in their eigenvalue spectrum. *SIAM J. Sci. Comput.* 24:1091–106
100. E W. 2003. Analysis of the heterogeneous multiscale method for ordinary differential equations. *Commun. Math. Sci.* 1:423–36
101. Engquist B, Tsai Y-H. 2005. Heterogeneous multiscale methods for stiff ordinary differential equations. *Math. Comput.* 74:1707–42
102. Vandekerckhove C, Roose D. 2008. Accuracy analysis of acceleration schemes for stiff multiscale problems. *J. Comput. Appl. Math.* 211:181–200
103. Rico-Martinez R, Gear CW, Kevrekidis IG. 2004. Coarse projective kMC integration: forward/reverse initial and boundary value problems. *J. Comput. Phys.* 196:474–89
104. Lee S, Gear CW. 2007. Second-order accurate projective integrators for multiscale problems. *J. Comput. Appl. Math.* 201:258–74
105. Abdulle A. Jan 2002. Fourth order Chebyshev methods with recurrence relation. *SIAM J. Sci. Comput.* 23:2041–54
106. Gear CW, Kevrekidis IG. 2003. Telescopic projective methods for parabolic differential equations. *J. Comput. Phys.* 187:95–109
107. Sommeijer BP. 1990. Increasing the real stability boundary of explicit methods. *Comput. Math. Appl.* 19:37–49
108. Vandekerckhove C, Roose D, Lust K. 2007. Numerical stability analysis of an acceleration scheme for step size constrained time integrators. *J. Comput. Appl. Math.* 200:761–77
109. Samaey G, Roose D, Kevrekidis IG. 2005. The gap-tooth scheme for homogenization problems. *SIAM Multiscale Model. Simul.* 4:278–306
110. Roberts AJ, Kevrekidis IG. 2005. Higher order accuracy in the gap-tooth scheme for large-scale dynamics using microscopic simulators. *ANZIAM J.* 46:C637–57
111. Li J, Kevrekidis PG, Gear CW, Kevrekidis IG. 2003. Deciding the nature of the "coarse equation" through microscopic simulations: the baby-bathwater scheme. *SIAM Multiscale Model. Simul.* 1:391–407
112. Samaey G, Kevrekidis IG, Roose D. 2006. Patch dynamics with buffers for homogenization problems. *J. Comput. Phys.* 213:264–87
113. Gear CW. 2001. Projective integration methods for distributions. *Tech. Rep. TR 2001-130*, NEC Res. Inst., Princeton, N.J.

99. Presents formulation and original stability analysis of projective integration methods.

111. Presents algorithms to obtain qualitative information on the coarse equation (order, conservative nature) useful in constructing, e.g., a patch dynamics scheme.

114. Erban R, Kevrekidis IG, Othmer H. 2006. An equation-free computational approach for extracting population-level behavior from individual-based models of biological dispersal. *Phys. D Nonlinear Phenom.* 215:1–24
115. Hadjiconstantinou NG. 1999. Hybrid atomistic-continuum formulations and the moving contact-line problem. *J. Comput. Phys.* 154:245–65
116. Samaey G, Roose D, Kevrekidis IG. 2006. Finite difference patch dynamics for advection homogenization problems. In *Model Reduction and Coarse-Graining Approaches for Multiscale Phenomena*, ed. AN Gorban, N Kazantzis, IG Kevrekidis, HC Öttinger, C Theodoropoulos, pp. 205–24. Berlin: Springer
117. Roberts AJ. 2002. A holistic finite difference approach models linear dynamics consistently. *Math. Comput.* 72:247–62
118. Roberts AJ, Kevrekidis IG. 2007. General tooth boundary conditions for equation free modelling. *SIAM J. Sci. Comput.* 29:1495–510
119. Carr J. 1981. *Applications of Centre Manifold Theory*. New York: Springer
120. Samaey G, Roberts AJ, Kevrekidis IG. 2008. Equation-free computation: an overview of patch dynamics. In *Bridging the Scales in Science and Engineering*, ed. J Fish. New York: Oxford Univ. Press. In press
121. Sankaranarayanan K, Shan X, Kevrekidis I. 1999. Bubble flow simulations with the lattice Boltzmann method. *Chem. Eng. Sci.* 54:4817–23
122. Theodoropoulos C, Sankaranarayanan S, Sundaresan S, Kevrekidis IG. 2001. Coarse bifurcation studies of bubble flow microscopic simulations. In *Proc. 3rd Pan-Hellenic Conf. Chem. Eng.*, ed. N Markatos, I Yentekakis, A Karabelas, S Bebelis, S Boghosian, et al., pp. 221–24. Athens: Cosmoware
123. Succi S. 2001. *The Lattice Boltzmann Equation for Fluid Dynamics and Beyond*. New York: Oxford Sci.
124. Sriraman S, Kevrekidis IG, Hummer G. 2005. Coarse nonlinear dynamics and metastability of filling-emptying transitions: water in carbon nanotubes. *Phys. Rev. Lett.* 95:130603
125. Sriraman S, Kevrekidis IG, Hummer G. 2005. Coarse master equation from Bayesian analysis of replica molecular dynamics simulations. *J. Phys. Chem. B* 109:6479–84
126. Hummer G, Rasaiah J, Noworyta J. 2001. Water conduction through the hydrophobic channel of a carbon nanotube. *Nature* 144:188–90
127. Larson RG, Scriven LE, Davis HT. 1985. Monte-Carlo simulation of model amphiphilic oil-water systems. *J. Chem. Phys.* 83:2411–20
128. Kopelevich DI, Panagiotopoulos AZ, Kevrekidis IG. 2005. Coarse-grained computations for a micellar system. *J. Chem. Phys.* 122:044907
129. Kopelevich D, Panagiotopoulos A, Kevrekidis I. 2005. Coarse-grained kinetic computations for rare events: application to micelle formation. *J. Chem. Phys.* 122:044908
130. Gear CW, Kevrekidis IG. 2004. Computing in the past with forward integration. *Phys. Lett. A* 321:335–43
131. Bold K, Zou Y, Kevrekidis I, Henson M. 2007. An equation-free approach to analyzing heterogeneous cell population dynamics. *J. Math. Biol.* 55:331–52
132. Moon S, Nabet B, Leonard N, Levin S, Kevrekidis IG. 2007. Heterogeneous animal group models and their group-level alignment dynamics: an equation-free approach. *J. Theor. Biol.* 246:100–12
133. Gross T, Kevrekidis IG. 2008. Robust oscillations in SIS epidemics on adaptive networks: coarse graining by automated moment closure. *Europhys. Lett.* 82:38004
134. Cisternas J, Gear CW, Levin S, Kevrekidis IG. 2004. Equation-free modeling of evolving diseases: coarse-grained computations with individual-based models. *Proc. R. Soc. Ser. A* 460:2761–79
135. Laing C, Frewen T, Kevrekidis I. 2007. Coarse-grained dynamics of an activity bump in a neural field model. *Nonlinearity* 20:2127–46
136. Szell A, Merritt D, Kevrekidis I. 2005. Core collapse via coarse dynamic renormalization. *Phys. Rev. Lett.* 95:081102
137. Erban R, Frewen TA, Wang X, Elston TC, Coifman R, et al. 2007. Variable-free exploration of stochastic models: a gene regulatory network example. *J. Chem. Phys.* 126:155103
138. Amat M, Kevrekidis I, Maroudas D. 2007. Coarse molecular-dynamics analysis of stress-induced structural transitions in crystals. *Appl. Phys. Lett.* 90:171910
139. Siettos CI, Armaou A, Makeev AG, Kevrekidis IG. 2003. Microscopic/stochastic timesteppers and coarse control: a kinetic Monte Carlo example. *AIChE J.* 49:1922–26

120. Contains details on patch dynamics, including a discussion of initial and boundary conditions for the patches, buffers, and convergence results.

140. Tenenbaum JB, de Silva V, Langford JC. 2000. A global geometric framework for nonlinear dimensionality reduction. *Science* 5500:2319–23
141. Belkin M, Niyogi P. 2003. Laplacian eigenmaps for dimensionality reduction and data representation. *Neural Comp.* 15:1373–96
142. Coifman R, Lafon S. 2006. Diffusion maps. *Appl. Comput. Harmon. A* 21:5–30
143. Nadler B, Lafon S, Coifman R, Kevrekidis IG. 2006. Diffusion maps, spectral clustering and reaction coordinates of dynamical systems. *Appl. Comput. Harmon. A* 21:113–27
144. Nadler B, Lafon S, Coifman R, Kevrekidis IG. 2006. Diffusion maps, spectral clustering and eigenfunctions of Fokker-Planck operators. In *Advances in Neural Information Processing Systems 18*, ed. Y Weiss, B Schölkopf, J Platt, pp. 955–62. Cambridge, MA: MIT Press
145. Simoncini V, Szyld DB. 2003. Theory of inexact Krylov subspace methods and applications to scientific computing. *SIAM J. Sci. Comput.* 25:454–77
146. Givon D, Kevrekidis IG. 2008. Multiscale integration schemes for jump-diffusion systems. *SIAM Multiscale Model. Simul.* 7:495–516
147. Gilbert N. 2007. *Agent-Based Models*. London: Sage
148. Grier DG. 2003. A revolution in optical manipulation. *Nature* 424:810–16
149. Gheorma IL, Haas S, Levi AFJ. 2004. Aperiodic nanophotonic design. *J. Appl. Phys.* 95:1420–26
150. Roslund J, Roth M, Rabitz H. 2006. Laboratory observation of quantum control level sets. *Phys. Rev. A* 74:043414

142. Diffusion maps can be used to obtain coarse variables from fine-scale simulation data; reviews diffusion maps and underlying principles.

Annual Review of
Physical Chemistry

Volume 60, 2009

Contents

Indexes

Errata

An online log of corrections to *Annual Review of Physical Chemistry* articles may be found at http://physchem.annualreviews.org/errata.shtml